Observation of Water Trees Using Terahertz Spectroscopy and Time-domain Imaging

Ryo Sato, Marina Komatsu, Yoshimichi Ohki
Department of Electrical Engineering and Bioscience, Waseda University.
3-4-1 Ohkubo, Shinjuku, Tokyo 169-8555, Japan

Norikazu Fuse
Central Research Institute of Electric Power Industry
2-6-1 Nagasaka, Yokosuka, Kanagawa 240-0196, Japan

Yoshinobu Nakamichi
Railway Technical Research Institute
2-8-38 Hikarichyo, Kokubunji, Tokyo 185-8540, Japan

Maya Mizuno and **Kaori Fukunaga**
National Institute of Information and Communications Technology
4-2-1 Nukuikitamachi, Koganei, Tokyo 184-8795, Japan

ABSTRACT

Terahertz measurements were carried out to detect water trees grown in low-density polyethylene sheets. Water absorbs light at terahertz frequencies, fairly strongly at about 5.0 THz and rather weakly from 0.1 to 1.0 THz. Using the absorption at these frequencies, observation of water trees was tried according to the following procedures. First, we made a model sample, consisting of a polyethylene sheet, a water layer, and a copper plate, and terahertz light was irradiated to this sample vertically. The waveform and intensity of electric field of the terahertz light reflected by the sample clearly pointed out the presence of water layer beneath the polyethylene sheet by the reflection peak appearance time and the phase of reflected electric field. Secondly, water trees were grown in a polyethylene sheet, and terahertz light was scanned over the sheet. As a result, the intensity distribution of terahertz light reflected by the sample was in good agreement with the shape of the water trees. Observation of terahertz image was also carried out using the same polyethylene sheet with water trees over which a polyvinyl chloride sheet or a carbon-loaded polyethylene sheet was put to simulate the structure of a real cable. An image of water trees was also successfully observed. These results indicate that the terahertz spectroscopy can be a new characterization tool to observe the presence of water trees in a test sample taken from an aged cable.

Index Terms — **Water tree, terahertz imaging, non-destructive analysis, insulation diagnosis.**

1 INTRODUCTION

IN high and medium voltage power cables or insulated wires, water trees may occur and grow when they are used under the presence of electric field and water [1-5]. Since cables or insulated wires with no water-shielding layers are still being used widely, detection of water trees is of prime importance for maintenance of such cables and wires. Although much research has been done [6-10], no truly reliable non-destructive methods to detect water trees have been established. Furthermore, it is often performed to observe water trees in an insulation material taken from field aged or laboratory aged cables, in order to understand how the degradation process proceeds. Optical microscopy is mainly used for such an observation, however, as direct observation provides no sufficient contrast, the specimen is usually stained before observation. This staining process is time consuming.

On the other hand, terahertz (THz) light with frequencies from about 0.1 to 10 THz have emerged as a new scientific tool. Thanks to recent advances in related science and technology, research applications of THz light have been expanded to much broader fields. For example, material analyses using THz

Manuscript received on 17 February 2011, in final form 7 June 2011.

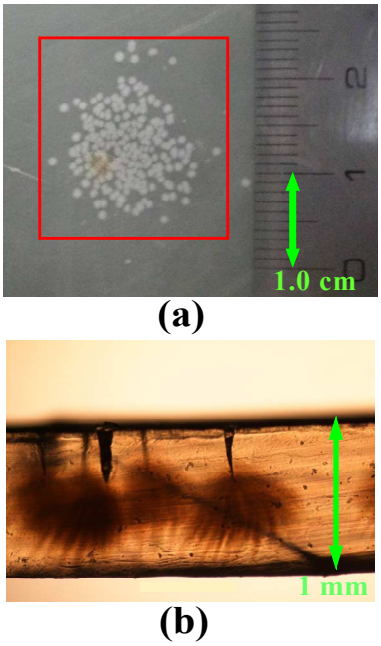

Figure 1. Views of sample T with water trees. A surface view taken by a digital camera (a) and a cross-sectional view by a polarization microscope (b). The frame shows the portion at which the imaging was carried out.

spectroscopy have been carried out for many substances such as electrical insulating materials, biodegradable polymers, pigments in western paintings and so on [11-17]. This attractive technique may provide an excellent tool for observation of water trees without staining process. In addition, as it provides spectrum in both time and frequency domains, much more useful information may be extracted from the dataset. In this paper, a fundamental study was conducted on the possibility of detection of water trees in polymeric electrical insulating materials using THz spectroscopy and imaging.

2 EXPERIMENTAL

The samples used are 1.0 mm thick low-density polyethylene (PE) sheets. While the as-received one is called sample A, the one with many pinholes having the average depth of ~300 μm filled with open air, made with a tungsten-carbide needle having a curvature-radius of 10 μm, is called sample H. The one with many similar pinholes filled with a NaCl solution of 0.1 mol/l is called sample W. Furthermore, a sheet of sample W was immersed in a NaCl solution of 0.1 mol/l, and an ac voltage (2 kHz, 3 kV) was applied for 168 hours at room temperature. Here, the pinholes filled with the NaCl solution in the sheet worked as water needle electrodes, from which water trees grew. This sheet is called sample T.

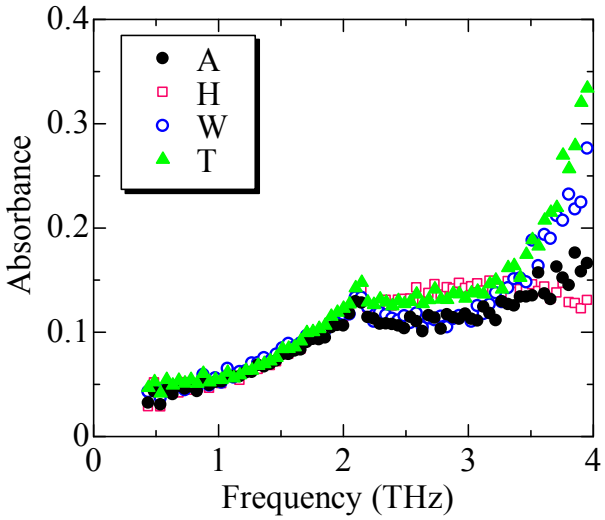

Figure 2. Absorption spectra of PE samples; sample A: as-received, sample H: with pinholes formed in open air, sample W: with pinholes formed in a NaCl solution, sample T: with water trees.

Furthermore, tests were conducted using layered samples consisting of one or two PE sheets, a water layer, and an aluminum or copper plate. More information such as the structure and the sheet and layer thicknesses will be mentioned when necessary.

For the above-mentioned samples, THz spectra were obtained in a frequency range from 0.4 to 4.0 THz in vacuum using a THz time-domain spectrometer (TDS: Tochigi Nikon, Rayfact Spectera; FWMH beam diameter ~3 mm at 0.3 THz), while absorption spectra were measured in a frequency range from 4.5 to 30 THz by a Fourier-transform infrared (FT-IR) spectrometer (Jasco VIR-F; FWMH beam diameter ~5 mm at 9 THz). Furthermore, reflective intensity distributions were

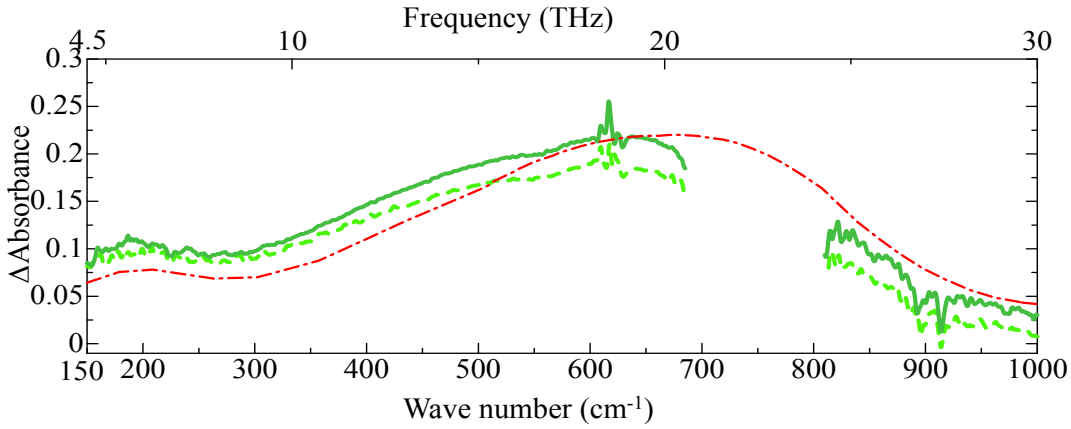

Figure 3. Differential FT-IR spectra of sample T obtained before and after a THz-TDS measurement by subtracting the spectrum of sample A. ——: before the THz-TDS measurement done in vacuum; — —: after the THz-TDS measurement, —·—: Absorbance of water reported in [19-21].

Table 1. Values of absorption coefficient, refractive index, and extinction coefficient at about 0.5 THz measured for each material constituting the samples.

	Absorption coefficient [cm^{-1}]	Refractive index	Extinction coefficient
Air	–	1	–
PE	0.5	1.5	~0
Polyvinylchloride	10	1.8	0.03
Carbon-loaded PE	~60	2	~0.3
Water [18, 19]	150	2.25	0.75
Copper [21]	–	31.6*	120*
Aluminum [21]	–	60.7*	147*

*values at 15 THz

obtained in a frequency range from 0.01 to 1.0 THz by a THz-TDS image scanner (Picometrix, T-Ray4000, FWHM beam diameter ~0.7 mm). All the measurements were carried out at room temperature in ambient atmosphere or in vacuum.

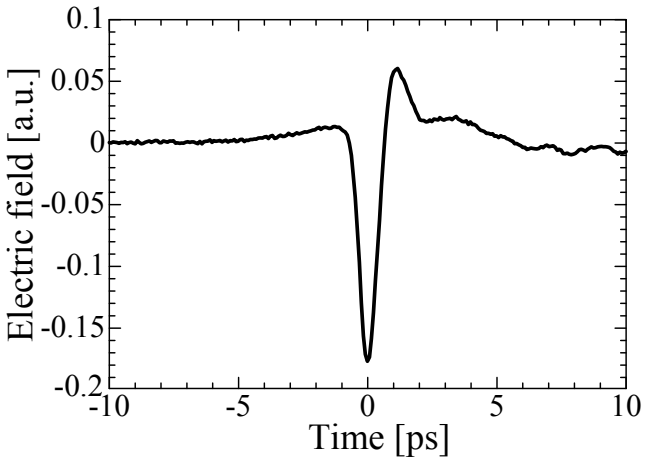

Figure 4. Electric field waveform of THz light reflected from the aluminum plate.

3 RESULTS AND DICUSSION

Figure 1 shows surface and cross-sectional views of sample T taken by a digital camera (a) and a polarization microscope (b), respectively. Water trees appear as white circles in the surface image (a) and as black shadows with the shape of a human hand in the cross-sectional image (b). The water tree length is about 500 μm.

First, THz-TDS measurements to obtain frequency spectra were carried out for samples A, H, W, and T at frequencies from 0.4 to 4.0 THz. Figure 2 shows the absorption spectra obtained by the measurements. A broad absorption band spreading over the whole measurement range with a peak at around 2.1 THz is observed in all the samples. While sample H with many open pinholes shows an absorption spectrum similar to that of sample A, two samples W and T containing water, namely W with water needles and T with water trees, show a clear absorption edge that increases its intensity with an increase in frequency toward 4.0 THz. This absorption edge seems to be due to resonance resulting from intermolecular vibration of water, which has been reported to have a peak at around 5.0 THz [18, 19]. Therefore, it is clearly demonstrated that the presence of water can be confirmed by THz spectroscopy.

However, the above-mentioned THz-TDS measurements were carried out while the samples were kept in a vacuum of 5.0×10^{-2} Pa. Therefore, a question may arise whether or not water actually remained inside the samples during the measurements. To examine this point, FT-IR spectra were observed. Namely, the IR measurement was conducted twice for sample T before and after the THz-TDS measurement, and the IR spectrum of sample A was subtracted from the two spectra of sample T in order to obtain differential absorption spectra that emphasize the absorption by water. In Figure 3, the differential absorption spectrum obtained before the THz-TDS measurement is denoted by the solid curve, while the one obtained after the measurement is denoted by the broken curve. The absorbance spectrum of water reported in [18-20] is also shown in Figure 3. The shape and frequency of the hump appearing in the two spectra observed in the sample at about 4.5 to 6 THz and those of the peak at 19 THz are in agreement with those of the absorption spectra of water [19, 20], if we ignore fine fluctuations or noises seen in almost the entire frequency range. Therefore, it was demonstrated that water remained in the sample after the THz-TDS measurements had been conducted in vacuum. Furthermore, it can be estimated from the value of differential absorbance that about 1.5×10^{-3} g/cm^3 of water remained in the sample T.

Next, THz imaging was tried using layered samples consisting of different materials, aiming at showing the possibility of detecting the existence of water or water trees in polymeric insulation. Table 1 shows the absorption coefficients, refractive indices, and damping coefficients of the constituent materials measured at around 0.5 THz [18, 19, 21]. The absorption of THz light is not so large except for water and carbon-loaded PE used as a semi-conductive layer and each material has a different refractive index and extinction coefficient. Therefore, it seems possible that THz light is reflected at the interface of different substances. This indicates that imaging is possible by the use of this reflection.

Figure 4 shows the electric field waveform of THz light reflected from the aluminum plate. The abscissa represents the sampling time or the time elapsed from the emission of the THz light pulse. Here, the time at which the reflection waveform returned from the aluminum plate was chosen as the base datum point. A large negative peak and a small positive peak appear at 0 and 1 ps, respectively. From here, all the waveforms observed by the experiments would be analyzed in reference to this waveform.

As a first trial, a model sample consisting of a PE sheet, a water layer, and a copper plate shown in Figure 5a, which simulates a polymeric insulating sheet with water trees grown inside was examined by scanning the power integrated over time. Figure 5b shows the time waveform of THz electric field reflected at points I, II, III, and IV on the sample. The reflection waveform observed at point I shows a large negative intensity with the phase opposite to that of the incident light. This means that the phase of electric field was

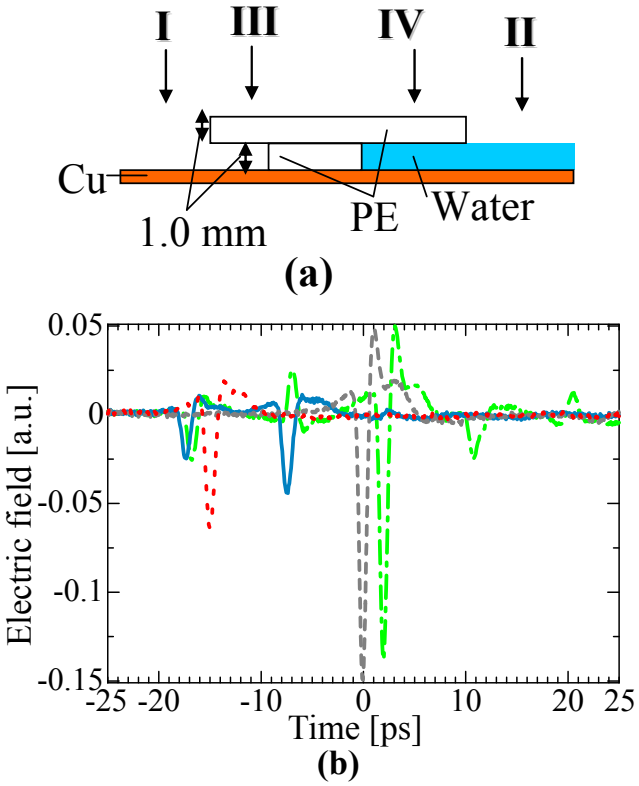

Figure 5. (a) Schematic of the model sample consisting of a PE sheet, a water layer, and a copper plate, used to simulate a water-tree degraded cable with a PE insulation. (b) Reflection waveforms of electric field obtained by shining the THz light beam at different points on the sample surface; — —: at point I (copper plate), ••••••: II (water layer), — · —: III (PE and air layer), ——: IV (PE and water layer).

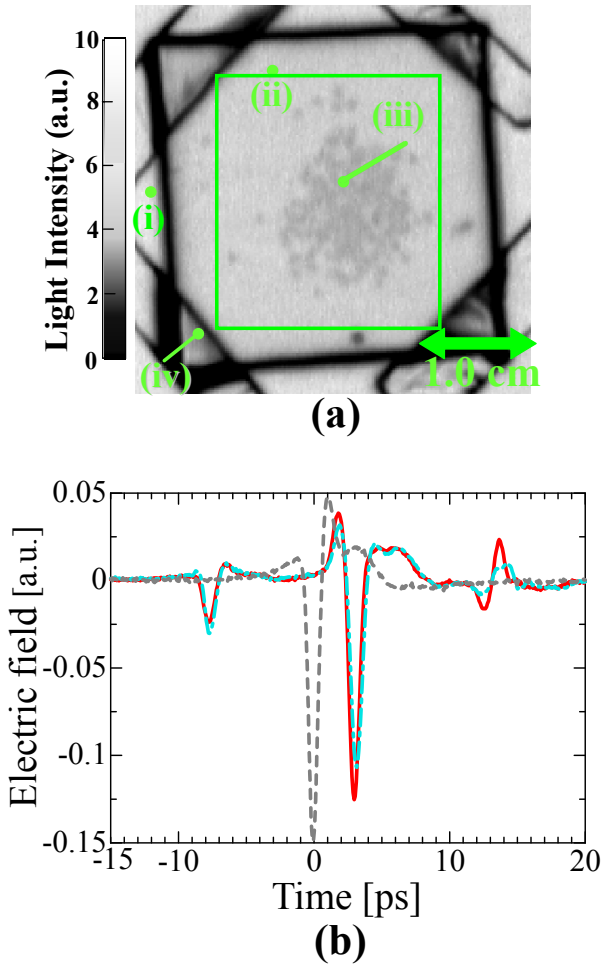

Figure 6. THz imaging of sample T with water trees. (a) Imaging result obtained by scanning the light intensity of THz light pulses reflected from the surface of the water-treed PE sheet shown in Figure 1a. The frame corresponds to the one in Figure 1a. The light intensity is indicated by colors; white, gray, and black. (b) Reflection waveforms of electric field obtained by shining the THz light beam at different points on the sample surface; — —: at point (i) (aluminum plate), ——: at point (ii) (PE with no water trees), — · —: at point (iii) (PE with water trees).

reversed upon the reflection on a substance with a higher refractive index than air. By taking the sampling time into account, it is clear that this reflection peak is due to the copper plate. In the waveforms observed at point II, only one reflection peak with the negative intensity appeared at -15 ps. This reflection occurred on the surface of water, which makes the peak appearance time earlier than that of the reflection on the copper surface at point I. On the other hand, five and two reflection peaks are observed in the waveforms at points III and IV, respectively. From the sampling time and the phase of each peak, the peaks at -17, -7, and 2 ps seem to be caused due to the reflection at the PE sheet, the air layer (in the case of point III) or the water layer (point IV), and the copper plate, respectively. While the last two peaks near 11 and 20 ps in the waveform at point III are caused by multiple reflection inside the sam ple. Here, as for the peak near -7 ps, the phase of electric field at point IV is opposite to the one at point III. The reason for this is that the refractive index of PE is higher than that of air and lower than that of water. Namely, the responses of the incident THz light pulse at points III and IV can distinguish the presence of water and air beneath the PE sheet with a thickness of 1.0 mm and those at points II and IV can also clearly demonstrate the position of the water surface. Here, peaks due to the reflection on the copper plate disappeared at points II and IV. This indicates that the absorption by water was too large. Therefore, the possibility was confirmed that the image of water trees can be traced using this method by scanning the reflection intensity.

As a next step, reflection measurements were carried out for sample T. Figure 6a shows the two dimensional intensity distribution of the THz light reflected from the surface of the water-treed PE sheet shown in Figure 1a. Here, the reflection intensity is strongest where the color is white and it becomes weaker in the order of gray and black. The black portion denoted as (iv) corresponds to the edge of sample T and adhesive tapes used to paste the sample on an aluminum plate. While the region enclosed by this black frame corresponds to sample T, the points (i), (ii), and (iii) correspond to the aluminum plate, the portion of sample T with no water trees, and the one with water trees, respectively. As mentioned above, gray means that the reflected THz electric field intensity is weak compared with the surrounding white portion. Note that the positions of light gray dots are completely in good agreement with those of water trees in the sample shown in Figure 1a. Moreover, Figure 6b shows

reflection waveforms of electric field observed at points (i), (ii), and (iii). Here, the time at which the reflection waveform returned at point (i) was chosen as the base datum point, and the electric field intensity is displayed as positive when it is with the same phase as the incident THz light pulse. In the reflection waveform (i), only one peak with a negative intensity is observed, which corresponds to the reflection on the aluminum plate. The waveforms (ii) and (iii) have three reflection peaks at -8, 3, and 13 ps. Based on the sampling time and the phase of each peak, they seem to be the reflection at the top surface of PE sheet, combination of reflection by air at the interface between the PE sheet and the aluminum plate (= the front low positive peak), reflection on the aluminum plate (= the next deep negative peak), and multiple reflection inside the sample, respectively. Note that the reflection by the aluminum plate appears later at points (ii) and (iii) than at (i) by the difference in refractive index between air and PE (or water). As for the combined positive and negative reflection at 2 to 3 ps that passed through the PE layer and the positive reflection at 13 ps caused by multiple reflection, their peak intensities are weaker at point (iii) than at point (ii). This fact also indicates the presence of water that absorbs THz light more than PE at point (iii). As a summary of the findings that can be obtained from Figure 6, the imaging of water trees in the top sheet or those grown from the sample surface is possible using THz light at frequencies from 0.01 to 1.0 THz.

As mentioned above, water trees in PE are detectable by THz light. Since insulating polymers are usually the outermost components of insulating wires, this method would be applicable without so much trouble. However, in a power cable, polymeric insulation in which water trees may be grown is always inside the cable, and the insulation is usually covered by a polymeric sheath made of polyvinyl chloride (PVC) and the like. Here, eye observation cannot detect water trees since PVC is opaque to visible light. In some cases, a semi-conductive layer is laid between the sheath and the insulation. Namely, it is impossible to shine THz light directly to the insulation. Therefore, in order to examine the applicability of this method to an actual cable as a non-destructive insulation diagnostic method, the detection of water trees was tried for samples covered by a sheath and a semi-conductive layer. First, the sample T was put on an aluminum plate and covered with a PVC sheath with a thickness of 312 μm, and THz imaging was tried in a similar way as in the case of Figure 6. Figure 7a shows the intensity distribution of the THz light reflected from the surface of water treed PE sheet shown in Figure 1a. The meanings of white, gray, and black in Figure 7a are the same as those in Figure 6a. Distribution of many gray dots showing lower field intensity is in good agreement with that of water trees shown in Figure 1a. This fact indicates that PVC is transparent enough in the THz region and that THz imaging of water trees is possible in polymeric insulation covered with a PVC sheath.

Figure 7b shows reflection waveforms of THz electric field observed at points (i), (ii), and (iii) on the sample. In addition to the peaks due to multiple reflection in the sample that appear at 16 ps and later, three reflection peaks are seen in the

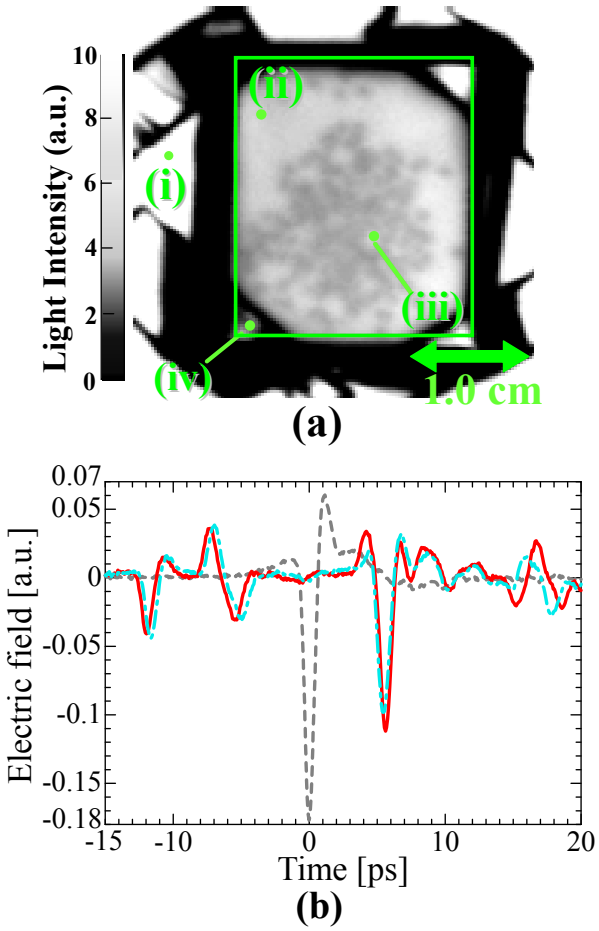

Figure 7. (a) THz imaging results obtained by scanning the light intensity of reflected THz light pulses over the surface of a PVC sheath, put on the surface of the water-treed PE sheet shown in Figure 1a. The frame corresponds to the one in Figure 1a. (b) Reflection waveforms of electric field obtained by shining the THz light beam at different points on the sample surface; — —: at point (i) (aluminum plate), ——: at point (ii) (PE with no water trees), —·—: at point (iii) (PE with water trees).

waveforms measured at points II and III. Based on the sampling time and phase of each peak, the peaks at -12, -8 to -5, and 6 ps seem to be caused by the reflection at the top surface of the PVC sheath, combination of the reflection at the interface between the PVC sheath and the air layer (= the positive peak at -7 ps) and reflection at the top surface of the PE sheet (= the negative one at -6 to -4 ps), and the reflection on the aluminum plate, respectively. Since the reflection caused by the PE sheet at -6 to -4 ps appeared, it is clear that the THz light passed through PVC. Furthermore, the electric field of the THz light pulse reflected on the aluminum plate, or the depth of the negative peak at 6 ps, is weaker when it was observed at point (iii) than it was observed at point (ii). The reason of this is that the THz light pulse attenuated more due to the presence of water at point (iii). This fact also indicates the possibility of detecting water or water trees by the THz imaging.

Similar measurements were repeated for sample T covered with a semi-conductive layer. Here, the semi-conductive layer was made by mixing carbon powder into PE, and its thickness was 84 μm. As shown in Table 1, the absorption in the semi-

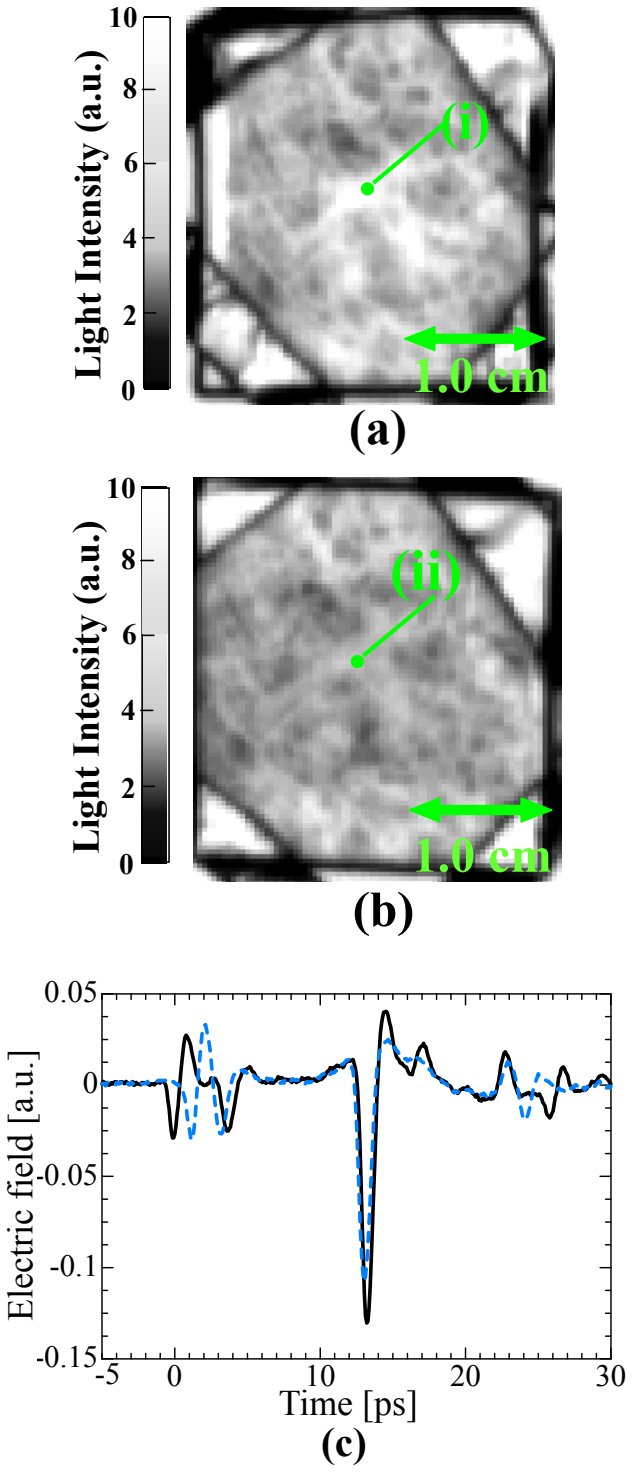

Figure 8. THz imaging results obtained by scanning the light intensity of reflected THz light pulses over the surface of a semi-conductive layer, put on a non-degraded PE sheet (a) or on a water-treed PE sheet (b). (c) Reflection waveforms of electric field obtained by shining the THz light beam at different points on the sample surface; ——: at point (i) (PE with no water trees), — —: at point (ii) (PE with water trees).

conductive layer is very strong. Therefore, subtle roughness or thickness dispersion of the layer exerts strong influence on the reflection waveform of THz light. For this reason, it was impossible to extract only the attenuation of the THz light due to water trees. The imaging experiment was also impossible to conduct. Therefore, a layered sample consisting of a non-degraded PE sheet covered with the semi-conductive layer and a similar one consisting of a PE sheet with water trees covered with the same semi-conductive layer were prepared, and the reflected light intensity was compared between the two.

Figure 8 shows the intensity distributions of the THz light reflected from the surface of water treed PE sheet shown in Figure 1a. The distributions for the non-degraded PE and water-treed PE are shown in Figures 8a and 8b, respectively. The meanings of the white, gray, and black are the same as those of Figures 6 and 7, and the black square corresponds to the edge of the sample. Intensity of the reflected light is not at all uniform even in Figure 8a that shows the result for the non-degraded PE, which is due to the above-mentioned effect of the strong absorption by semi-conductive layer. Moreover, compared to Figure 6, the intensity of the reflected light is very weak in both Figures 8a and 8b, because of the strong absorption by the semi-conductive layer. When we compare Figures 8a and 8b, the intensity is much weaker in Figure 8b. There is a high possibility that the absorption of THz light by water in water trees is responsible for this difference in intensity.

In order to confirm this assumption, reflection waveforms of electric field intensity were obtained at point (i) in Figure 8a and at point (ii) in Figure 8b that are the same position on the samples. In the waveforms shown in Figure 8c, three sets of reflection peak groups are seen. From the sampling time and the phase of each peak, the reflection that caused each peak can be estimated. The first peak group appearing at 0 to 4 ps seems to be caused by the reflection at the top surface of the semi-conductive layer (= the first negative peak), at its bottom surface (= the second positive one), and at the top surface of the PE sheet (= the third negative one). The peak groups at 12 to 15 ps and at 22 to 24 ps are due to the reflection on the aluminum plate and multiple reflection inside the sample, respectively. If we compare the intensity of the first peak group at points (i) and (ii), the intensities of the black solid curve representing the intensity at point (i) and the blue broken curve representing the intensity at point (ii) are approximately the same at around 0 to 4 ps. However, as for the second peak group at about 12 to 15 ps, the broken curve is smaller than the solid one. This means that the peak at point (ii) is weak compared with the one at point (i) at around 12 to 15 ps. This indicates that the THz light was damped by the water inside the water trees. This in turn indicates that imaging of water trees is possible even if the polymeric insulation is covered with a substance like semi-conductive polymer with a high absorption coefficient as long as the reflected THz light keeps its intensity strong enough to be measurable by a detector.

In order to further confirm the above, the imaging was carried out by extracting only the light from ~22 to 23 ps shown in Figure 8c, or the light detected after the multiple reflection inside the PE sample with water trees. Figures 9a and 9b show the imaging results or the intensity distributions of the multi-reflected light obtained using the waveforms observed for the non-degraded sheet and water-treed sheet, respectively. As in the case of previous figures, the intensity is

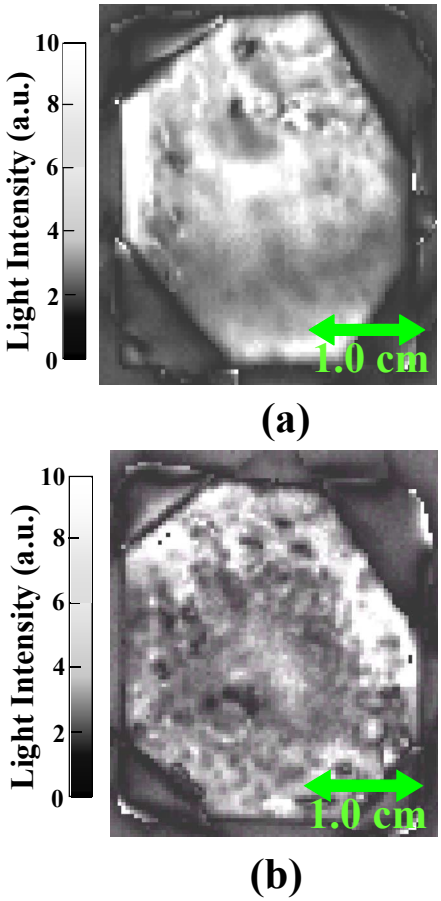

Figure 9. THz imaging results obtained by scanning the intensity of multi-reflected THz light in a time period from ~22 to 23 ps shown in Figure 8c over the surface of the semi-conductive layer, put on the non-degraded PE sheet (a) or on the water-treed PE sheet (b).

strongest where the color is white, and it becomes weaker in the order of gray and black. More black dots are seen in Figure 9b than in Figure 9a, and their positions agree with the positions of water trees. It seems that Figure 9 gives a clearer image than Figure 8, since the attenuation due to the presence of water is enhanced by the multiple reflections.

All the results mentioned-above indicate that the present technique can provide a good tool to observe the presence of water trees in a test sample taken from a field-aged or laboratory-aged cable. However, it is true that much research must be done and some technological breakthroughs are definitely needed before this technique can be applied to a real cable with a metallic shield tape or wire.

4 CONCLUSIONS

Terahertz measurements were carried out to study the possibility of detection of water trees grown in polyethylene. As a result, the following findings were obtained.

1. An absorption edge that increases its intensity with an increase in frequency toward 4.0 THz appears in a sample with water trees. This is attributable to the presence of water inside the sample.
2. Distribution of water trees grown from the surface of a polymer or those present in an underneath polymer were successfully imaged using THz light at frequencies from 0.01 to 1.0 THz.
3. Imaging of water trees is possible even if the polymeric insulation is covered with a substance like a polyvinyl chloride sheath or semi-conductive polymer with a high absorption coefficient as long as the reflected THz light keeps its intensity strong enough to be measurable by a detector.

REFERENCES

[1] H. Suzuki, S. Mukai, Y. Ohki, Y. Nakamichi, and K. Ajiki, "Water-tree characteristics in low-density PE under simulated inverter voltages", IEEE Trans. Dielectr. Electr. Insul., Vol. 5, pp. 256-260, 1998.

[2] T. Toyoda, S. Mukai, Y. Ohki, Y. Li, and T. Maeno, "Estimation of conductivity and permittivity of water trees in PE from space charge distribution measurements", IEEE Trans. Dielectr. Electr. Insul., Vol. 8, pp. 111-116, 2001.

[3] D. Kaneko, T. Maeda, T. Ito, Y. Ohki, T. Konishi, Y. Nakamichi, and M. Okashita, "Role of number of consecutive voltage zero-crossings in propagation of water trees in polyethylene", IEEE Trans. Dielectr. Electr. Insul., Vol. 11, pp. 708-714, 2004.

[4] T. Maeda, D. Kaneko, Y. Ohki, T. Konishi, Y. Nakamichi, and M. Okashita, "Voltage zero-crossing as a factor inducing water trees", IEEJ Trans. Fundam. Mater., Vol. 125, pp. 51-56, 2005.

[5] Y. Ohki, "Aiming at a more rigorous understanding in electrical insulating materials research," IEEE Trans. Dielectr. Electr. Insul., Vol. 15, pp. 1201-1214, 2008.

[6] L. Tommasino, "Solid dielectric detectors with breakdown phenomena and their applications in radioprotection", Nucl. Instr. and Meth., Vol. 173, pp. 73-83, 1980.

[7] H. M. Li, R. A. Fouracre, and B. H. Crichton, "Transient current measurement for the detection of water tree growth in polymeric power cables", IEEE Trans. Dielectr. Electr. Insul., Vol. 2, pp. 866-874, 1995.

[8] R. Patsch and J. Jung, "Water trees in cables: generation and detection", IEE Proc.-Sci. Meas. Technol., Vol. 146, pp. 253-259, 1999.

[9] P. Werelius, P. Thärning, R. Eriksson, B. Holmgren, and U. Gäfvert, "Dielectric spectroscopy for diagnosis of water tree deterioration in XLPE cables", IEEE Trans. Dielectr. Electr. Insul., Vol. 8, pp. 27-42, 2001.

[10] Y. Ohki, "News from Japan, A novel water-tree detection method for XLPE power cable", Electr. Insul. Mag., Vol. 20, pp. 54–55, 2004.

[11] Y. Ohki, M. Okada, N. Fuse, K. Iwai, M. Mizuno, and K. Fukunaga, "Terahertz time-domain spectroscopic analysis of molecular behavior in polyamide nanocomposites", Appl. Phys. Express, Vol. 1, pp. 122401 1-3, 2008.

[12] Y. Ohki, M. Okada, N. Fuse, K. Iwai, M. Mizuno, and K. Fukunaga, "Terahertz spectroscopy as a new analyzing tool for dielectric properties of various insulating materials", IEEE Conf. Electr. Insul. Dielectr. Phenomena (CEIDP), pp. 33-36, 2008.

[13] B. Ferguson and X. Zhang, "Materials for terahertz science and technology", Nat. Mater., Vol. 1, pp. 26-33, 2002.

[14] T. D. Dorney, R. G. Baraniuk, and D. M. Mittleman, "Material parameter estimation with terahertz time-domain spectroscopy", J. Opt. Soc. Am. A, Vol. 18, pp. 1562-1571, 2001.

[15] U. Møller, D. G. Cooke, K. Tanaka, and P. U. Jepsen, "Terahertz reflection spectroscopy of Debye relaxation in polar liquids", J. Opt. Soc. Am. B, Vol. 26, No. 9, pp. 113-125, 2009.

[16] K. Fukunaga, N. Sekine, I. Hosako, N. Oda, H. Yoneyama, and T. Sudou, "Real-time terahertz imaging for art conservation science", J. Eur. Opt. Soc. Rap. Public., Vol. 3, pp. 1-4, 2008.

[17] N. Fuse, R. Sato, M. Mizuno, K. Fukunaga, K. Ito, and Y. Ohki, "Observation and analysis of molecular vibration modes in polylactide at terahertz frequencies", Jpn. J. Appl. Phys., Vol. 49, pp. 102402 1-8, 2010.

[18] C. Zhang, K. S. Lee, X. C. Zhang, X. Wei, and Y. R. Shen, "Optical constants of ice Ih crystal at terahertz frequencies", Appl. Phys. Lett., Vol. 79, pp. 491-493, 2001.
[19] S. G. Warren, "Optical constants of ice from the ultraviolet to the microwave", Appl. Opt., Vol. 23, pp. 1206-1225, 1984.
[20] M. R. Querry, D. M. Wieliczka, and D. J. Segelstein, "Water (H_2O)", in *Handbook of Optical Constants of Solids II*, E. D. Palik, ed. (Academic, Boston, Mass., 1991), pp. 1059-1077.
[21] M. A. Ordal, L. L. Long, R. J. Bell, S. E. Bell, R. R. Bell, R. W. Alexander, Jr., and C. A. Ward, "Optical properties of the metals Al, Co, Cu, Au, Fe, Pb, Ni, Pd, Pt, Ag, Ti, and W in the infrared and far infrared", Appl. Opt., Vol. 22, pp. 1099-1119, 1983.

Ryo Sato was born on 9 October 1987 in Tokushima, Japan. He received the B. Eng. degree from Waseda University in 2010 and is presently a graduate student.

Marina Komatsu was born on 16 August 1988 in Tokyo, Japan. She received the B. Eng. degree from Waseda University in 2011 and is presently a graduate student.

Norikazu Fuse was born on 5 April 1980 in Tokyo, Japan. He received the B.Eng., M.Eng., and Dr. Eng. degrees in 2003, 2005, and 2009, respectively, all from Waseda University. He was a Research Fellow of the Japan Society for the Promotion of Science from 2005 to 2008, a Research Associate of Waseda University from 2008 to 2010, a Guest Researcher of the National Institute of Information and Communication Technology (NICT) from 2009 to 2010, and is currently a Research Scientist of Central Research Institute of Electric Power Industry.

Yoshinobu Nakamichi was born on 19 January 1951 in Nagasaki, Japan. He received the B. Eng and M. Eng degrees in electronic engineering in 1973 and 1975, respectively, from Kyushu University. He also received the M.S. degree from Carnegie Mellon University in 1981 and Dr.Eng. degree from Waseda University in 2000. He joined the Japanese National Railways in 1975 and moved to Railway Technical Research Institute in 1987, where he is currently a Principal Researcher of Research & Development Promotion Division.

Maya Mizuno received her Ph.D. degree in engineering from Tohoku University in 2006 while she was working at RIKEN. She is presently a Researcher in the Applied Electromagnetic Research Center of NICT.

Kaori Fukunaga received her Ph.D. in engineering from Tokyo Denki University in 1993 while she was working at Fujikura Ltd. She joined the NICT in 1994, and is a Research Manager in the Applied Electromagnetic Research Center. She is a member of IEEE, IIC and IEEJ.

Yoshimichi Ohki (M'76-SM'98-F'00) received the B.Eng., M.Eng. and Dr. Eng. degrees in 1973, 1975 and 1978, respectively, all from Waseda University, Japan. He joined the teaching staff of the Department of EE, Waseda University in 1976 and is presently a Professor. He was a Visiting Scientist at the Massachusetts Institute of Technology from 1982 to 1984. He is a recipient of the Forster, Whitehead, and Ieda Awards from IEEE-DEIS, Outstanding Achievement Award and two Best Paper Awards from IEE Japan, and other awards. His major research interests cover various organic and inorganic dielectrics, e.g., those used in optical fibers and power cables.